Supporting Information

Ultra-fast Vapor Generation by a Graphene Nano-ratchet: a Theoretical and Simulation study

Hongru Ding[1,2,#], Guilong Peng[1,2,#], Shenqiu Mo[1,2], Dengke Ma[1,2], S.W. Sharshir[1,2] and Nuo Yang[1,2,*]

[1]State Key Laboratory of Coal Combustion, Huazhong University of Science and Technology (HUST), Wuhan 430074, P. R. China

[2]Nano Interface Center for Energy(NICE), School of Energy and Power Engineering, Huazhong University of Science and Technology (HUST), Wuhan 430074, P. R. China

[#] H. D. and G. P. contributed equally to this work.

Electronic mail: N.Y. (nuo@hust.edu.cn)

SI. Molecular dynamic simulation details

<table>
<tr><td>Method</td><td colspan="6">Non- Equilibrium MD</td></tr>
<tr><td colspan="7">Potential</td></tr>
<tr><td>Function</td><td colspan="6">$E = \sum_{i}^{on\ a} \sum_{j}^{on\ b} \frac{k_c q_i q_j}{r_{ij}} + \frac{A}{r_{oo}^{12}} - \frac{B}{r_{oo}^{6}} + 4\epsilon[(\frac{\sigma}{r})^{12} - (\frac{\sigma}{r})^{6}]$</td></tr>
<tr><td rowspan="4">Parameters
(TIP4P)</td><td>m_O</td><td colspan="2">m_H</td><td>q_M (C)</td><td>q_H (C)</td><td>R_{OM} (Å)</td><td>$R_{coul,cut}$ (Å)</td></tr>
<tr><td>15.999</td><td colspan="2">1.008</td><td>-1.040</td><td>0.520</td><td>0.15</td><td>8.5</td></tr>
<tr><td>R_{OH} (Å)</td><td>θ_{OH} (°)</td><td colspan="2">$A \times 10^{-3}$ (Kcal Å^{12}/(mol))</td><td colspan="2">B (Kcal Å^6/(mol))</td><td></td></tr>
<tr><td>0.9572</td><td>104.52</td><td colspan="2">600.0</td><td colspan="2">610.0</td><td></td></tr>
<tr><td rowspan="3">Parameters
(VDW)</td><td>Type of molecular</td><td>N_2^*</td><td>O_2^*</td><td colspan="2">C</td><td colspan="2" rowspan="3">*Two centered LJ potential for N_2 and O_2</td></tr>
<tr><td>ϵ (Kcal/(mol*Å^2))</td><td>0.0725</td><td>0.1034</td><td colspan="2">0.05528</td></tr>
<tr><td>Σ (Å)</td><td>3.32</td><td>2.99</td><td colspan="2">3.415</td></tr>
<tr><td colspan="7">Simulation process</td></tr>
<tr><td>Ensemble</td><td colspan="5">Setting</td><td>Purpose</td></tr>
<tr><td rowspan="4">NVT</td><td>Time step (fs)</td><td>1</td><td>Runtime (ns)</td><td colspan="2">3</td><td rowspan="4">Relax structure</td></tr>
<tr><td>Temperature (K)</td><td>300</td><td>Thermostat</td><td colspan="2">Nosé–Hoover</td></tr>
<tr><td>Simulation cell (nm)</td><td colspan="4">13.6*12.2*22</td></tr>
<tr><td>Boundary condition</td><td colspan="4">X, Y, Z:
periodic, periodic, fixed</td></tr>
<tr><td rowspan="3">NVT</td><td>Runtime (ns)</td><td>8</td><td>Temperature (K)</td><td colspan="2">300</td><td rowspan="3">Record information</td></tr>
<tr><td>Simulation cell (nm)</td><td colspan="4">13.6*12.2*22</td></tr>
<tr><td>Boundary condition</td><td colspan="4">X, Y, Z:
periodic, periodic, fixed</td></tr>
</table>

SII. Test of timestep

In molecular dynamic simulations, the timestep size is constrained by the demand that the vibrational motion of the atoms be accurately tracked. Usually, timestep is limited to femtosecond scale [1]. To perform accurate but economic simulations, we made a test about different timesteps. We fix N_l, A_{min} and $\tan\alpha$ as 3, 33.1Å^2 and 0.25, in this part. We calculate the pressure difference of MGCN with different timesteps at room temperature, the results are shown in Fig S1. The values of ΔP change little when the timesteps are smaller than 1 fs. It shows that our simulation cell is large enough to overcome the finite size effect on calculating thermal conductivity. In all of the simulations of MGCN, we use 1 fs as the timestep.

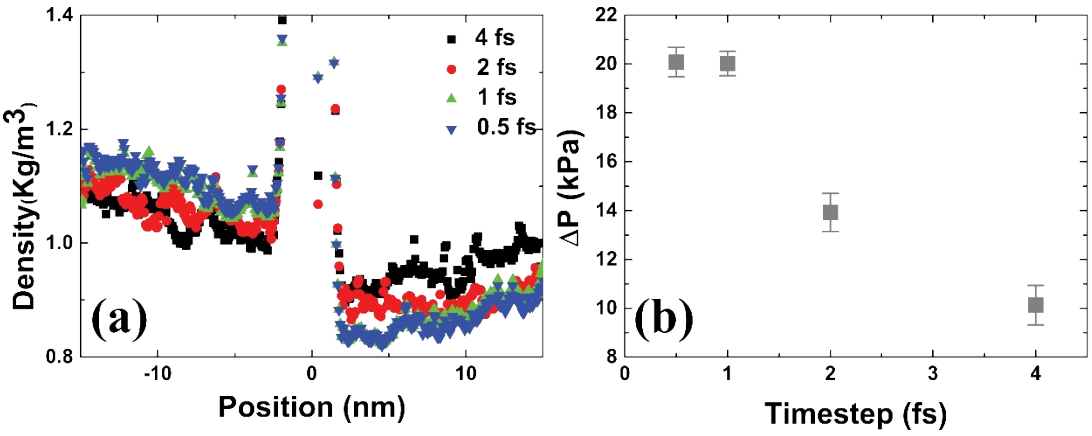

Figure S1. The density profile of saturated moist air molecules (a) and the pressure difference (b) with different timesteps. In this simulation, MGCN is constructed by 3 layers' graphene with cone-shaped nanopores. The area of minimum pore is 33.1 Å^2 and the cone angle α is $arctan_{0.25}$.

SIII. Finite size effect

In this simulation, the finite size effect could arise if the simulation cell is not sufficiently large. As shown in Figure S2, we calculate the pressure difference ΔP of MGCN with different sizes at room temperature. We fix the number of graphene layers N_l, the area of the minimum pore A_{min} and the cone angle α as 2, 33.1Å^2 and arctan0.25, respectively. The values of ΔP change little when the size of simulation cell is larger than 4×4 unit cells (UCs). It shows that our simulation cell is large enough to overcome the finite size effect on calculating ratchet transport. In all of the simulations of MGCN, we use 4×6 UCs as simulation cell.

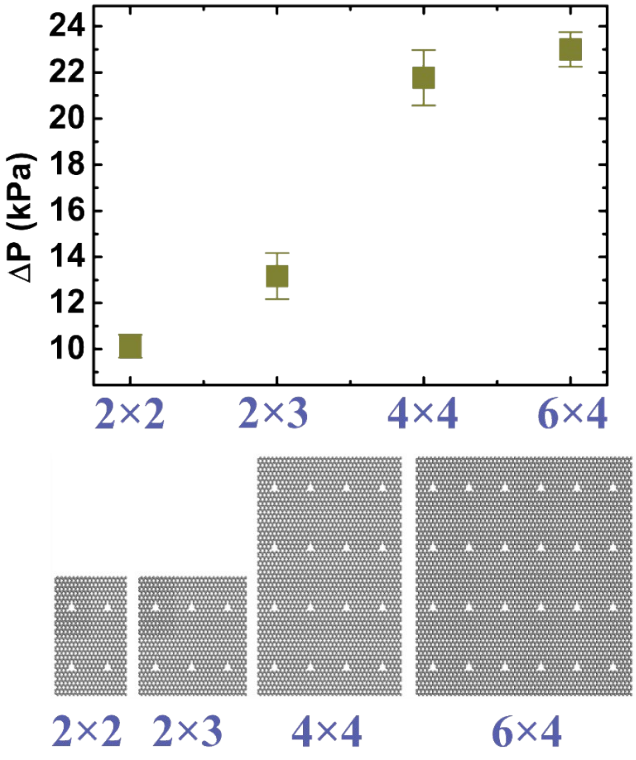

Figure S2. The pressure difference versus simulation cells. In this simulation, MGCN is constructed by 2 graphene layers with cone-shaped nanopores, where the area of minimum pore is 33.1 Å^2 and the cone angle α is $arctan0.25$.

SIV. Dependence of ambient temperature

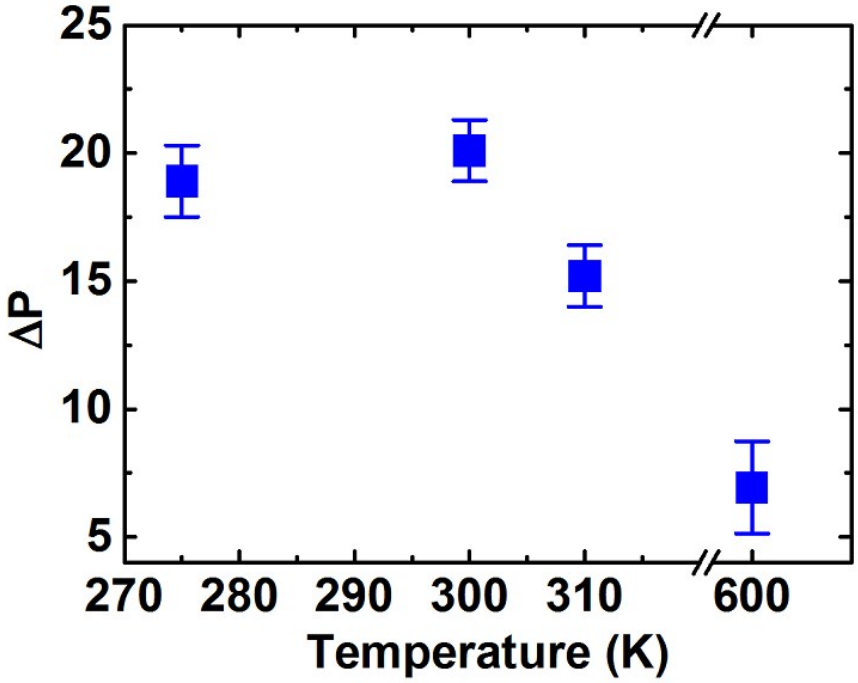

Figure S3. The pressure difference versus ambient temperature. ΔP shows a significant reduction, when ambient temperature increase from 300 K to 600 K. In this simulation, MGCN is constructed by 4 graphene layers with cone-shaped nanopores, where the area of minimum pore is 55.2 $Å^2$ and the cone angle α is $arctan0.25$.

SV. Dependence of cone angle α

ΔP also has nonmonotonic dependence on the cone angle α. In the following cases, N_l and A_{min} are fixed as 3 and 33.1 $Å^2$, respectively. As shown in Fig. 2(d), we get the biggest ΔP, 20.1 kPa, when tanα is 0.25. Figure S4 shows the force distribution of MGCN with different α. As for the reasons of the low ΔP for the other three α: on the one hand, the narrow nanochannel and many energy barriers of the small-α MGCN confine the ratchet effect; On the other hand, the strong diffusion transport and weak negative force of the big-α MGCN result in the low ΔP. The discussions about diffusion transport are described in details below. That is why the adopted tanα of other simulations is fixed at 0.25 in this paper.

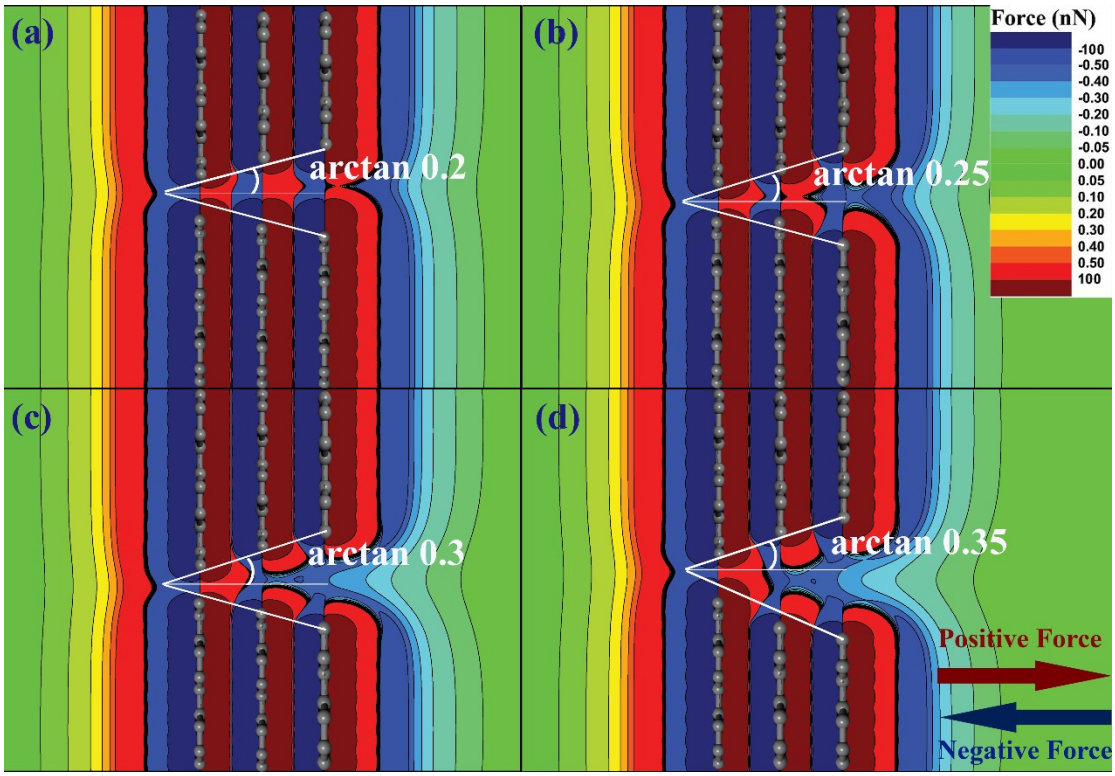

Figure S4. The number of graphene layers is fixed as 3; and the area of minimum pore A_m as 33.1 $Å^2$. The force (along the Z direction) distribution of MGCN with different cone angle, $arctan_{0.2}$- $arctan_{0.35}$, are shown in (a)-(d). The arrows point out the

direction of positive and negative force.

SVI. Knudsen Diffusion

Diffusive transport, resulted from the concentration difference, also affects the molecular transport. The molecules will move from the high concentration region to the low due to the diffusive transport, and this limits the further growth of concentration. Therefore, the final distribution of air depends on the competition between the ratchet transport (leftward) and diffusive transport (rightward). Since the scale length of the cone-shaped nanopores is much smaller than the mean free path of the air molecules, the Knudsen diffusion [2] occurs here. The Knudsen diffusion flux is defined as,

$$\Phi_k = -\frac{2}{3}\bar{r}u\frac{dC}{dz} \tag{S1}$$

$$\bar{r} = (r_{min} + r_{max})/2 \tag{S2}$$

$$r_{max} = r_{min} + (N_l - 1)htan\alpha \tag{S3}$$

where $\bar{r}$ is the mean radium of the nanochannel, r_{min} and r_{max} are radiuses of the minimum and maximum pores. r_{min} equals to $\sqrt{A_{min}/\pi}$; u is the characteristic velocity of air molecules; $\frac{dC}{dz}$ is the concentration gradient and h is the interlayer spacing of MGCN. In equation (S1), $\bar{r}$ and Φ_k are substituted by (S2)-(S3). Then equation (S1) can be defined as,

$$\Phi_K = -\frac{2r_{min} + (N_l - 1)htan\alpha}{3}u\frac{dC}{dz} \tag{S4}$$

SVII. Evaporation enhancement calculation

According to Hertz-Knudsen Relation [3] as defined here:

$$\dot{m} = (\sigma_e \frac{P_S}{\sqrt{T_L}} - \sigma_c \frac{P_V}{\sqrt{T_a}}) \sqrt{\frac{M}{2\pi R}} \tag{S5}$$

where $\dot{m}$ is the evaporation rate of the water, P_S and P_V are the water vapor saturate pressure and the real vapor partial pressure at the interface respectively. σ_e and σ_c are the evaporation and condensation coefficient, respectively. M is the molar mass of the water molecule. T_L and T_a are the temperature of the water and vapor at the interface respectively.

Normally, σ_e and σ_c are measured at the range of 0.001 to 1 and very close to each other [3-5]. T_L is slightly higher than T_a when water is heated to evaporate.[6] And P_V is lower than P_S due to the lower vapor temperature and molecular diffusion. Therefore, the following assumptions are made: (i) The temperature discontinuity at the water-vapor interface is ignored, i.e., $T_L = T_a = T$; (ii) The difference between evaporation and condensation coefficient is ignored, i.e., $\sigma_e = \sigma_c = \varepsilon$.

when MGCN is applied, the enhancement of evaporation, η_i, can be calculated as:

$$\eta_i = \frac{P_V - P_V^{'}}{(P_S - P_V)} \times 100\% \tag{S6}$$

where $P_V^{'}$ and P_V are the real vapor saturate pressure at the interface with and without MGCN respectively. According to equation (1), P_V can be described as:

$$P_V = P_S - \frac{\dot{m}}{\varepsilon} \sqrt{\frac{2\pi RT}{M}} \tag{S7}$$

Meanwhile, as shown in Figure S4, due to the diffusion resistance, the vapor would accumulate on the high pressure side, which indicates that the pressure on the high pressure side of MGCN can be regarded as P_S. Therefore, $P_V^{'}$ can be determined by:

$$P_V^{'} = \left(1 - \frac{\Delta P}{P_{atm}}\right) P_S \tag{S8}$$

where P_{atm} is the atmospheric pressure, ΔP is the pressure difference between the two sides of MGCN. Hence, η_i can be described as:

$$\eta_i = \left(\frac{\varepsilon \cdot \Delta P \cdot P_S}{P_{atm}\dot{m}} \sqrt{\frac{M}{2\pi RT}} - 1\right) \times 100\% \tag{S9}$$

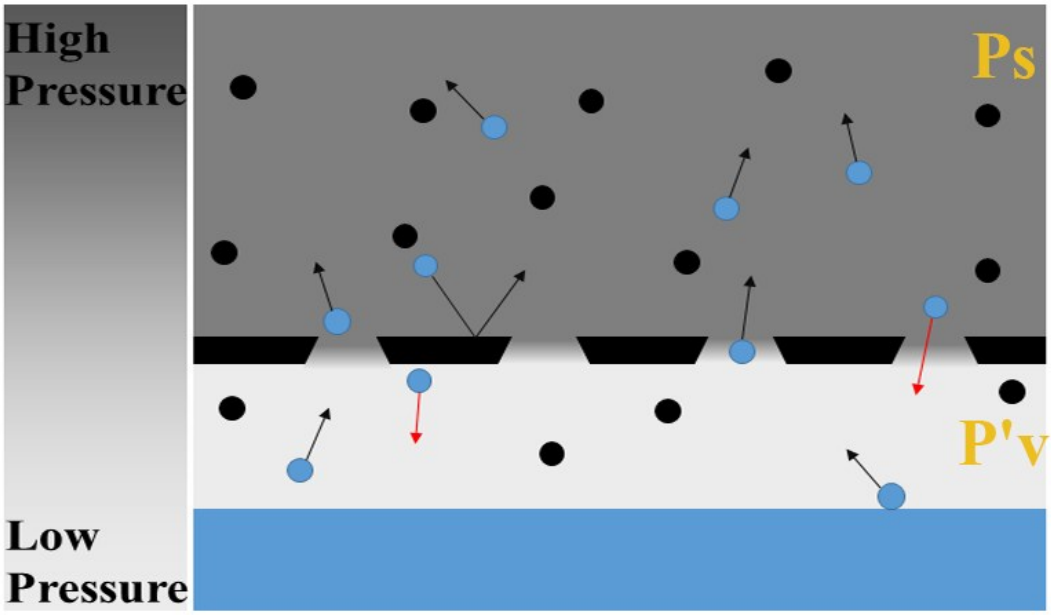

Figure S5. Vapor pressure on both sides of MGCN. The pressure at the interface, $P_V^{'}$, is low due to the pumping by MGCN, the pressure on the other side is P_S due to the accumulation of vapor molecules.

SVIII. Effect of pore chemistry

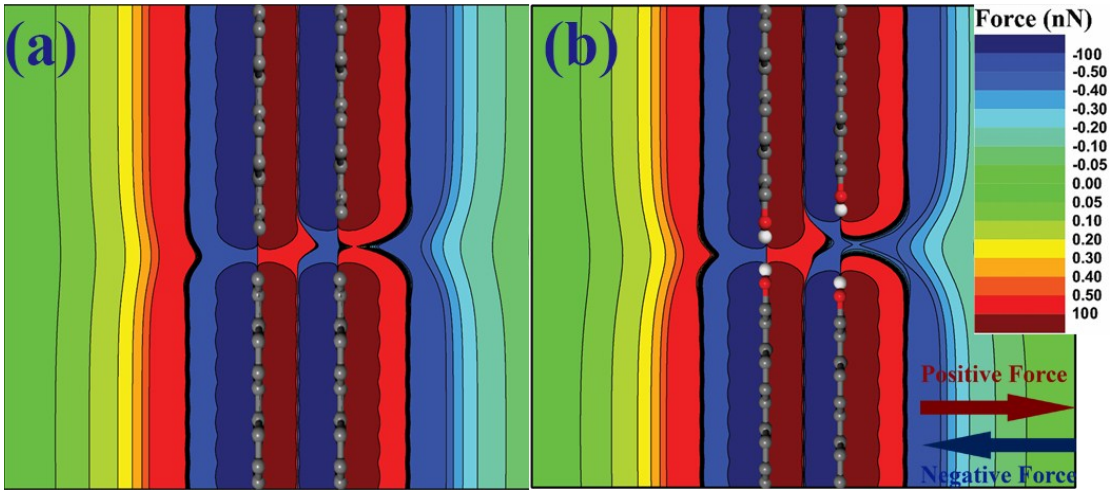

Figure S6. The force (along the Z direction) distributions of MGCN without (a) and with (b) hydroxyl groups. The number of graphene layers is 2. The area of minimum pore is 33.1 $Å^2$ and the cone angle is arctan0.25. The arrows point out the direction of positive and negative forces. The carbon (grey), oxygen (red) and hydrogen (white) atoms are shown to facilitate observation.

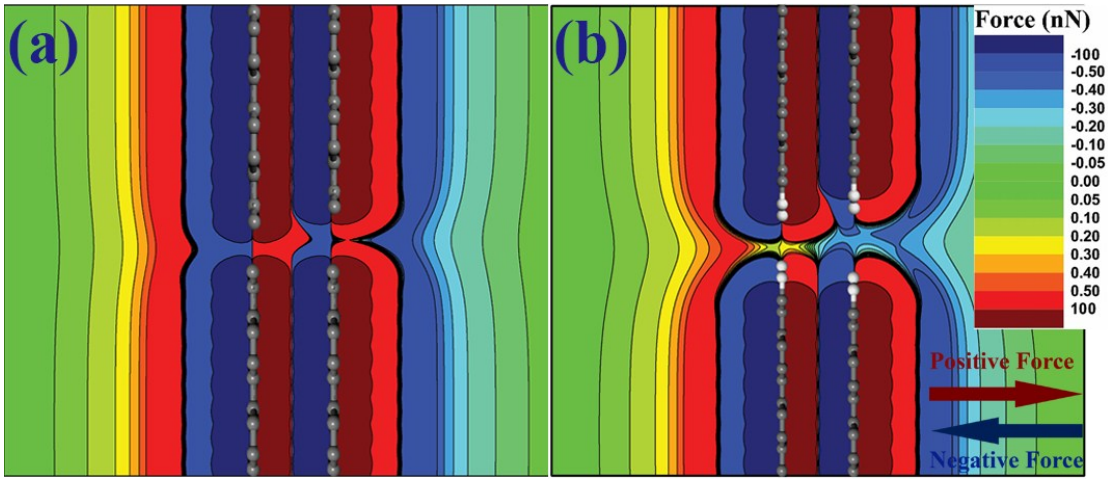

Figure S7. The force (along the Z direction) distributions of MGCN without (a) and with (b) hydrogen atoms. The number of graphene layers is 2. The area of minimum pore is 33.1 $Å^2$ and the cone angle is $arctan$0.25. The arrows point out the direction of positive and negative forces. The carbon (grey) and hydrogen (white) atoms are shown to facilitate observation.

Reference

[1] S. Plimpton, J. Comput. Phys., 1995, **117**, 1.

[2] M. Knudsen, Ann. d. Phys., 1909, **333**,75.

[3] A. H. Persad and C. A. Ward, Chem. Rev., 2016, **116**, 7727.

[4] I. W. Eames, N. J. Marr, and H. Sabir, Int. J. Heat mass tran., 1997, **40**, 2963.

[5] R. Marek and J. Straub, Int. J. Heat mass tran., 2001, **44**, 39.

[6] E. Y. Gatapova, I. A. Graur, O. A. Kabov, V. M. Aniskin, M. A. Filipenko, F. Sharipov and L. Tadrist, Int. J. Heat Mass Tran., 2017, **104**, 800.